J. Fluid Mech. (2014), *vol.* 748, *pp.* 328–349.
doi:10.1017/jfm.2014.190

The detrimental effect of hydrodynamic interactions on the process of Brownian flocculation in shear flow

Krzysztof A. Mizerski†

Department of Magnetism, Institute of Geophysics, Polish Academy of Sciences, ul. Ksiecia Janusza 64, 01-452 Warsaw, Poland

(Received 9 October 2013; revised 21 February 2014; accepted 3 April 2014; first published online 29 April 2014)

The problem of Brownian flocculation of spherical particles in strong shearing flow without hydrodynamic interactions is studied in detail using the singular perturbation method. All other types of interparticle interactions, such as van der Waals or Lennard-Jones forces, are also ignored. In the limit of strong external flow, the strength of which is measured by the Péclet number ($Pe \gg 1$), a complicated boundary layer structure for the pair probability density function (P_2) is identified and the complete stationary spatial distribution of $P_2(\boldsymbol{x})$ in the domain is found. The results, in particular the total mass flux in the accumulation process, are compared qualitatively and quantitatively with the case where the spheres interact hydrodynamically and it is demonstrated that the hydrodynamic interactions tend to decrease the rate of flocculation. An explicit simple formula for the flocculation rate for a general form of hydrodynamic interactions is provided. The limit of small Péclet number is also discussed to confirm the conclusion on the detrimental influence of hydrodynamic interactions on the rate of Brownian flocculation in shearing flow.

Key words: general fluid mechanics, particle/fluid flows, suspensions

1. Introduction

The problem of spontaneous Brownian flocculation of spherical particles in infinite space was first addressed by Smoluchowski (1917). Due to numerous occurrences in industry (e.g. production of cheese, application of paints, water treatment) and biology (aggregation of polymers), this problem has attracted a great deal of attention and has been developed to include additional effects present in real situations such as external flow and hydrodynamic interactions between particles in some simplified forms. In particular, polymer aggregation is a phenomenon that commonly occurs in many vital biological processes. One example is plugging of vascular injuries, where the blood flow unfolds the polymer chains, which then create a net for accumulation of platelets. Other examples involve the development of Alzheimer's and Parkinson's diseases. In all these examples the influence of the external flow is crucial. The first efforts were simply confined to the study of a uniform velocity field at infinity (e.g. Acrivos & Taylor 1962) and Frankel & Acrivos (1968) were the first to provide analytical results for weak Stokes shearing flow around a sphere, i.e. Stokes flow satisfying no-slip

† Email address for correspondence: kamiz@igf.edu.pl

impermeable boundary conditions at the central sphere and attaining shear flow form at infinity with a magnitude small compared with the diffusive effects (i.e. small Péclet number *Pe*). Batchelor (1979) by use of boundary layer theory generalized the results to any steady Stokesian flow around the central spherical particle that is linear in coordinates at infinity. In particular, the straining motion was analysed in detail in the limits of large and small *Pe*. Noh, Koh & Kang (1998) investigated numerically the shape of a growing particle for different types of straining flows and for arbitrary Péclet number. The hydrodynamic interactions were included in a numerical investigation by Zinchenko & Davis (1995) (see also the references therein) via the exact mobility formulae for the two-particle hydrodynamics and near-contact asymptotics (see e.g. Kim & Karrila 2005). To the best of the author's knowledge the issue of how the hydrodynamic interactions modify the process of Brownian flocculation has never been addressed, since the problem without any hydrodynamic interactions, i.e. pure shear flow everywhere in space, has never been resolved and direct comparison has not been possible. Moreover, the presence of potential forces between particles which is typically assumed in the literature strongly regularizes the problem. Here, we neglect any types of interactions between particles other than the hydrodynamic interactions; in particular, the regularizing influence of potential forces (e.g. van der Waals, Lennard-Jones) is ignored. The need for such a clear study, resolving solely the issue of the effect of the hydrodynamic interactions on the flocculation process, mainly comes from the numerous simulations of this process in biological fluid dynamics, where the hydrodynamic interactions are often neglected but their influence on the final result is far from obvious.

Here, we fill this gap and determine the influence of hydrodynamic interactions on the Brownian flocculation process, i.e. the concentration distribution and the flocculation rate. To this end we must first resolve the problem without hydrodynamic interactions, and then that solution is compared with that of the two-particle hydrodynamic mobility functions (see e.g. Russel, Saville & Showalter 1989) and the relation between the flocculation rates in the two cases is determined. Two limits, namely $Pe \gg 1$ and $Pe \ll 1$, are studied, to isolate the effects of streamline divergence and the decrease of diffusion with decreasing interparticle distances that result from hydrodynamic interactions.

The paper is structured as follows. First, we mathematically formulate the problem in § 2. Next, using the method of matched asymptotic expansions, which in the limit $Pe \gg 1$ considered in § 3 is simply the boundary layer theory, we find an asymptotic solution for the concentration field and determine the flocculation rate in agreement with previously obtained results. At the end of § 3 we analyse the problem in which hydrodynamic interactions are present and show that the flocculation rate is decreased by their presence. In particular, § 3.2.1 is dedicated to the study of a general form of hydrodynamic interactions, with a tunable degree of their strength. Section 4 is devoted to the small Péclet number limit, where we also prove the detrimental influence of hydrodynamic interactions on the rate of flocculation. We end with concluding remarks in § 5.

2. Mathematical formulation

For a detailed description of the dynamics of a suspension consisting of N identical spheres immersed in a fluid the probability density function $P_N(\boldsymbol{x}_1, \ldots, \boldsymbol{x}_N, t)$ is introduced, which specifies the probability of finding spheres centred simultaneously at $(\boldsymbol{x}_1, \ldots, \boldsymbol{x}_N)$, with the normalization $\int P_N \, \mathrm{d}\boldsymbol{x}_1 \ldots \mathrm{d}\boldsymbol{x}_N = N!$ (cf. Russel *et al.* 1989).

The function P_N possesses the information about the microstructure of the suspension; for example, the local number density can be expressed as

$$C(\boldsymbol{x}_1) = \frac{1}{(N-1)!}\int P_N \mathrm{d}\boldsymbol{x}_2 \ldots \mathrm{d}\boldsymbol{x}_N. \tag{2.1}$$

However, typically much less information is required than that possessed in the function P_N and it is often sufficient to consider the pair probability density function

$$P_2(\boldsymbol{x}_1, \boldsymbol{x}_2, t) = \frac{1}{(N-2)!}\int P_N \mathrm{d}\boldsymbol{x}_3 \ldots \mathrm{d}\boldsymbol{x}_N. \tag{2.2}$$

In particular, this is the case for dilute suspensions, i.e. small volume fractions $4\pi a^3 C/3 \ll 1$, where a is the radius of the spheres. In the absence of any interactions between the aggregating particles other than hydrodynamic interactions, which in general may be present, the standard conservation law for the function P_2 takes the form (cf. Russel *et al.* 1989)

$$\frac{\partial P_2(\boldsymbol{r}, t)}{\partial t} + \nabla \cdot [\boldsymbol{V}(\boldsymbol{r}) P_2(\boldsymbol{r}, t) - \boldsymbol{D}(\boldsymbol{r}) \cdot \nabla P_2(\boldsymbol{r}, t)] = 0, \tag{2.3}$$

where $\boldsymbol{r} = \boldsymbol{x}_2 - \boldsymbol{x}_1$, $\boldsymbol{D}(\boldsymbol{r})$ is the diffusion matrix (related to the mobility matrix $\boldsymbol{\mu}$, which is an inverse of the friction matrix, via the fluctuation–dissipation theorem, $\boldsymbol{D} = k_B T \boldsymbol{\mu}$, where T is the temperature and k_B is the Boltzman constant) and $\boldsymbol{V}(\boldsymbol{r})$ is the relative velocity of particles. We consider shearing flow of the form

$$\boldsymbol{v} = \boldsymbol{G} \cdot \boldsymbol{r} = \begin{bmatrix} 0 & 0 & 0 \\ 0 & 0 & 0 \\ \dot{\gamma} & 0 & 0 \end{bmatrix} \begin{bmatrix} x \\ y \\ z \end{bmatrix} = \dot{\gamma} x \hat{\boldsymbol{e}}_z, \tag{2.4}$$

where $\boldsymbol{G}$ is the velocity gradient tensor and $\dot{\gamma}$ is the constant rate of shear. Following Batchelor & Green (1972) (see also Russel *et al.* 1989) the velocity $\boldsymbol{V}$ takes the form

$$\boldsymbol{V}(\boldsymbol{r}) = \boldsymbol{G} \cdot \boldsymbol{r} - \boldsymbol{C}(\boldsymbol{r}) \cdot \boldsymbol{G}^{(s)} \cdot \boldsymbol{r}, \tag{2.5}$$

where the superscript (s) denotes symmetrization and $\boldsymbol{C}(\boldsymbol{r})$ is known as the shear disturbance tensor (and is directly linked to a component of the mobility matrix typically denoted by $\boldsymbol{\mu}^{td}$), which describes the influence of the particles on the flow of the suspension. Here, $\boldsymbol{C}(\boldsymbol{r})$, just like the diffusion matrix $\boldsymbol{D}(\boldsymbol{r})$, can take different forms, depending on the chosen level of approximation for the hydrodynamic interactions. In particular, when the hydrodynamic interactions are neglected the tensor $\boldsymbol{C}(\boldsymbol{r}) = \boldsymbol{0}$ and the diffusion is a unitary matrix, $\boldsymbol{D}(\boldsymbol{r}) = \boldsymbol{1}$.

As is typical in the study of Brownian flocculation, we pick one sphere to be located at the centre $\boldsymbol{r} = 0$ and seek the distribution of $P_2(\boldsymbol{r})$ in the domain $2a \leqslant r < \infty$ (note that in this case $P_2(\boldsymbol{r})$ is, in fact, the same as the concentration $C(\boldsymbol{r})$). Thus, the following boundary conditions are imposed for the problem of spontaneous aggregation in shear flow:

$$P_2(r = 2a) = 0 \quad \text{and} \quad P_2(r \longrightarrow \infty) = C_0, \tag{2.6a,b}$$

where C_0 is the concentration at infinity of a spatially homogeneous microstructure and the condition $P_2(r = 2a) = 0$ denotes irreversible flocculation.

We will be concerned with the stationary problem, thus $\partial P_2/\partial t = 0$. By assuming a and C_0 for the scales of length and the the pair probability density function respectively, the stationary equation can be made dimensionless and reads

$$Pe\boldsymbol{U}\cdot\nabla P_2 - \nabla\cdot[\boldsymbol{\mathcal{D}}\cdot\nabla P_2] = 0, \tag{2.7}$$

where Pe is the Péclet number (cf. Russel *et al.* 1989) and

$$Pe = \frac{\dot\gamma a^2}{D_0}, \quad D_0 = \frac{k_B T}{3\pi\eta a}, \quad \boldsymbol{V} = \dot\gamma a\boldsymbol{U}, \quad \boldsymbol{D} = D_0\boldsymbol{\mathcal{D}}, \tag{2.8a–d}$$

where η is the viscosity of the fluid. The boundary conditions in the dimensionless form are

$$P_2(r=2) = 0 \quad \text{and} \quad P_2(r\longrightarrow\infty) = 1. \tag{2.9a,b}$$

We also assume throughout the paper that the Reynolds number $Re = \rho\dot\gamma a^2/\eta \ll 1$, so that the Stokes flow approximation remains valid. The dimensional mass flux towards the central particle, in other words the rate of coagulation, is defined as follows:

$$J = 4D_0C_0a\int \mathrm{d}\Omega\boldsymbol{n}\cdot\boldsymbol{\mathcal{D}}\cdot\nabla P_2|_{r=2}, \tag{2.10}$$

where Ω is the solid angle; thus, the integration is carried out over the surface of the sphere $r=2$ and $\boldsymbol{n}$ is the unit normal. It should be noted that the advective term makes no contribution because of the imposed absorbing boundary condition $P_2(r=2)=0$.

3. The limit of large Péclet number, $Pe \gg 1$

3.1. *Flocculation without hydrodynamic interactions*

First, we study in detail the problem of aggregation of non-interacting hydrodynamically spherical particles. Physically, this corresponds to very porous particles; to imagine such a system one could think of spheres made of wire suspended in a fluid, which may flow relatively freely through the particles. In this case $\boldsymbol{C}(\boldsymbol{r}) = \boldsymbol{0}$ and $\boldsymbol{D}(\boldsymbol{r}) = \boldsymbol{1}$ (unitary matrix); thus, (2.7) reads

$$Pex\partial_z P_2 - \nabla^2 P_2 = 0, \tag{3.1}$$

with the boundary conditions given in (2.9).

In the limit of large Péclet number, $Pe \gg 1$, we apply the standard boundary layer theory. The mainstream problem outside the boundary layers is dominated by advection; thus, at leading order we obtain (cf. (3.1))

$$\boldsymbol{v}\cdot\nabla P_2^M = 0 \quad \text{or} \quad x\partial_z P_2^M = 0, \tag{3.2a,b}$$

so that the mainstream solution is constant on the streamlines (which are parallel to the z axis), and since the far-field boundary condition is $P_2^M(r\longrightarrow\infty)=1$ we obtain

$$P_{2,I}^M = 1 \tag{3.3}$$

everywhere in the mainstream in regions I (see figure 1). The regions II, in fact, do not span to infinity, since the two bounding boundary layers thicken with distance

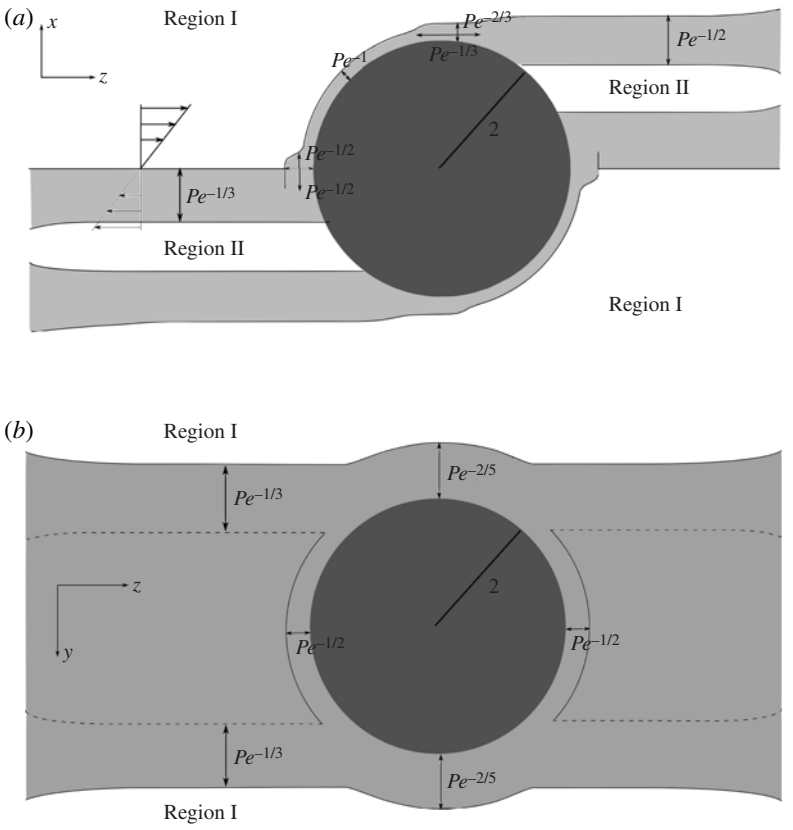

FIGURE 1. The schematic boundary layer structure in the spatial distribution of the probability density function $P_2(\boldsymbol{r})$: (*a*) in the *XZ* plane, (*b*) in the *YZ* plane.

from the central particle and eventually meet. Therefore, the absorbing boundary condition determines the solution in these regions, where

$$P^M_{2,II} = 0. \tag{3.4}$$

To resolve the boundary layers on the sphere we need to write down (3.1) in spherical coordinates,

$$v_r \frac{\partial P_2}{\partial r} + \frac{v_\theta}{r}\frac{\partial P_2}{\partial \theta} - \frac{1}{Pe}\left[\frac{1}{r^2}\frac{\partial}{\partial r}\left(r^2\frac{\partial P_2}{\partial r}\right) + \frac{1}{r^2\sin\theta}\frac{\partial}{\partial\theta}\left(\sin\theta\frac{\partial P_2}{\partial\theta}\right) + \frac{1}{r^2\sin^2\theta}\frac{\partial^2 P_2}{\partial\phi^2}\right] = 0, \tag{3.5}$$

where

$$v_r = r\sin\theta\cos\theta\cos\phi, \quad v_\theta = -r\sin^2\theta\cos\phi. \tag{3.6a,b}$$

Due to the symmetry of the problem it is sufficient to concentrate on the upper half-sphere $-\pi/2 \leqslant \phi \leqslant \pi/2$ (and then the solution for the lower half-sphere can be easily reproduced). On introducing the boundary layer variable

$$\xi = \frac{r-2}{\delta}, \tag{3.7}$$

we may rewrite (3.5) in the following form:

$$\begin{aligned} 0 \;=\; & \frac{(2+\xi\delta)}{\delta}\sin\theta\cos\theta\cos\phi\frac{\partial P_2^{BL}}{\partial\xi} - \sin^2\theta\cos\phi\frac{\partial P_2^{BL}}{\partial\theta} - \frac{1}{Pe\delta^2}\frac{\partial^2 P_2^{BL}}{\partial\xi^2} \\ & - \frac{1}{Pe\delta}\frac{2}{2+\xi\delta}\frac{\partial P_2^{BL}}{\partial\xi} - \frac{1}{Pe}\frac{1}{(2+\xi\delta)^2\sin\theta}\frac{\partial}{\partial\theta}\left(\sin\theta\frac{\partial P_2^{BL}}{\partial\theta}\right) \\ & - \frac{1}{Pe}\frac{1}{(2+\xi\delta)^2\sin^2\theta}\frac{\partial^2 P_2^{BL}}{\partial\phi^2}. \end{aligned} \tag{3.8}$$

The superscript *BL* is used throughout the text to denote the boundary layer function, i.e. function dependent on the boundary layer variable/variables. The structure and length scales of the boundary layers that form in the spatial distribution of the probability density function $P_2(\boldsymbol{r})$ are presented in figure 1. They will be resolved in the following sections.

3.1.1. *The $\delta \sim Pe^{-1}$ boundary layer*

Outside the neighbourhood of $(r=2,\ \theta=\pi/2)$, $(r=2,\ \theta=\pi)$ and $(r=2,\ \phi=\pm\pi/2)$ the distinguished balance in the boundary layer includes the dominant advective term and the dominant diffusive term, and thus yields

$$2\sin\theta\cos\theta\cos\phi\frac{\partial P_2^{BL}}{\partial\xi} - \frac{\partial^2 P_2^{BL}}{\partial\xi^2} = 0 \tag{3.9}$$

and

$$\delta = Pe^{-1}. \tag{3.10}$$

The solution satisfying the absorbing boundary condition on the sphere, $P_2(r=2)=0$, and matching the mainstream solution as $\xi \longrightarrow +\infty$ is

$$P_2^{BL} = 1 - \mathrm{e}^{v_{r0}\xi} = 1 - \mathrm{e}^{\sin 2\theta\cos\phi\xi}, \tag{3.11}$$

where $v_{r0} = 2\sin\theta\cos\theta\cos\phi$ is the value of the radial velocity component at the surface of the sphere. Of course, a solution of this form can only be matched with the mainstream solution for $\pi/2 < \theta < \pi$ (or in the lower half-plane for $\pi/2 \leqslant \phi \leqslant 3\pi/2$ and $0 < \theta < \pi/2$), i.e. on the side where the flow is hitting the sphere surface, and on the other side, where the flow leaves the sphere, there is no boundary layer, thus the pair probability density function (concentration) must vanish at least in some finite region past the sphere (namely region II). It remains to determine what happens in the regions that have been left out, i.e. in the vicinity of $(r=2,\ \theta=\pi/2)$, $(r=2,\ \theta=\pi)$ and $(r=2,\ \phi=\pm\pi/2)$, or in other words to resolve all the remaining boundary layers in the problem. However, as will become evident later, the $\delta \sim Pe^{-1}$ boundary layer is the thinnest of all the boundary layers at the sphere, thus it determines the leading-order average flux, J_0, towards the central particle

$$\begin{aligned} J_0 \;&=\; -8D_0C_0a\int_{-\pi/2}^{\pi/2}\mathrm{d}\phi\int_{\pi/2}^{\pi}\mathrm{d}\theta\sin\theta\left.\frac{\partial P_2}{\partial r}\right|_{r=2} \\ &=\; -8PeD_0C_0a\int_{-\pi/2}^{\pi/2}\mathrm{d}\phi\int_{\pi/2}^{\pi}\mathrm{d}\theta\sin\theta\left.\frac{\partial P_2^{BL}}{\partial\xi}\right|_{\xi=0} \\ &=\; 16PeD_0C_0a\int_{-\pi/2}^{\pi/2}\mathrm{d}\phi\int_{\pi/2}^{\pi}\mathrm{d}\theta\sin^2\theta\cos\theta\cos\phi = -\tfrac{32}{3}PeD_0C_0a, \end{aligned} \tag{3.12}$$

which agrees with the ballistic result of Levich (1962).

3.1.2. *The boundary layer at* $(r=2,\ \theta=\pi/2)$

At $\theta=\pi/2$ the normal component of the velocity vanishes, implying singularity in the boundary layer and thus different spatial scales. In the vicinity of $\theta=\pi/2$ we introduce a new variable

$$\vartheta=\frac{\pi/2-\theta}{\delta_\vartheta}\Longrightarrow\theta=\pi/2-\vartheta\delta_\vartheta, \tag{3.13}$$

where $\delta_\vartheta\ll 1$ defines the span of the singular boundary layer in the meridional direction, and expand

$$\sin\theta=1-\tfrac{1}{2}\left(\vartheta\delta_\vartheta\right)^2+\mathrm{O}\left(\delta_\vartheta^4\right),\quad \cos\theta=\vartheta\delta_\vartheta+\mathrm{O}\left(\delta_\vartheta^3\right). \tag{3.14a,b}$$

By introducing the new variable, i.e. (3.13) and (3.14), into (3.8) we get the following distinguished dominant balance:

$$2\vartheta\cos\phi\frac{\partial P_2^{BL}}{\partial\xi}+\cos\phi\frac{\partial P_2^{BL}}{\partial\vartheta}-\frac{\partial^2 P_2^{BL}}{\partial\xi^2}=0, \tag{3.15}$$

with

$$\delta=Pe^{-2/3},\quad \delta_\vartheta=Pe^{-1/3}. \tag{3.16a,b}$$

A change of variables

$$\vartheta=\frac{\tau}{\cos^{1/3}\phi},\quad \xi=\frac{\kappa}{\cos^{2/3}\phi} \tag{3.17a,b}$$

and

$$P_2^{BL}=1-\mathrm{e}^{\kappa\tau-\tau^3/3}\Psi\left(\kappa,\tau\right) \tag{3.18}$$

leads to the following equation for $\Psi(\kappa,\tau)$:

$$\frac{\partial^2\Psi}{\partial\kappa^2}-\kappa\Psi=\frac{\partial\Psi}{\partial\tau}. \tag{3.19}$$

The boundary conditions are written down for the pair probability density function

$$P_2^{BL}\left(\kappa\longrightarrow\infty,\tau\right)=1, \tag{3.20a}$$
$$P_2^{BL}\left(\kappa=0,\tau\right)=0, \tag{3.20b}$$
$$P_2^{BL}\left(\kappa,\tau\longrightarrow-\infty\right)=1, \tag{3.20c}$$

where the last condition (3.20*c*) comes from matching with the $\delta\sim Pe^{-1}$ boundary layer, already solved in the previous section. Interestingly, the same boundary layer problem was obtained in a quite different physical configuration of magneto-hydrodynamic channel and Couette flows with singular boundary layers of Hartmann type by Roberts (1967) and Dormy, Jault & Soward (2002). We will briefly summarize the method of solving (3.19) with (3.20*a*)–(3.20*c*) in appendix A, where the asymptotic form for $\tau\gg 1$ is also obtained. The solutions are of the form

$$\Psi=\Psi_{-1}+\Psi_0+\Psi_1, \tag{3.21}$$

where

$$\Psi_n=\int_0^\infty\frac{\mathrm{Ai}(\sigma)\mathrm{Ai}(\kappa+\omega^n\sigma)}{\mathrm{Ai}(\omega^n\sigma)}\exp(\omega^n\tau\sigma)\mathrm{d}\sigma. \tag{3.22}$$

It is a simple task to introduce the solution (3.21) and (3.22) into (3.19) to verify that it satisfies the boundary layer equation. By the use of (A 3) and (A 6) this solution easily satisfies the boundary conditions (3.20*b*) and (3.20*a*). On the other hand, the asymptotic (κ, τ)-dependence as $-\tau \gg 1$ can be readily obtained from (3.15) and (3.17), $P_2^{BL}(\kappa, \tau \to -\infty) \sim 1 - \mathrm{e}^{2\tau\kappa}$, which is the exact form of the solution of the $\delta \sim Pe^{-1}$ boundary layer achieved for $\theta - \pi/2 \sim Pe^{-1/3}$, thus the matching is correct. Moreover, it will prove to be useful later to also provide the asymptotic (κ, τ)-dependence for $\tau \gg 1$, which is (see appendix A)

$$P_2^{BL}(\kappa, \tau \gg 1) \sim \frac{1}{2}\mathrm{erfc}\left(\frac{\tau^2 - \kappa}{\sqrt{4\tau}}\right). \tag{3.23}$$

3.1.3. *The upper boundary layer past the sphere*

It is now convenient to switch to cylindrical polar coordinates (s, ϕ, z) and, by defining the boundary layer coordinate as

$$\zeta = \frac{s-2}{\delta}, \tag{3.24}$$

obtain the dominant distinguished balance in the boundary layer past the sphere in the vicinity of $r = 2$, which spans from $z = 0$ to infinity (for $z > 0$ above region II in figure 1*a*),

$$\frac{\partial^2 P_2^{BL}}{\partial \zeta^2} - 2\cos\phi \frac{\partial P_2^{BL}}{\partial z} = 0, \tag{3.25}$$

for

$$\delta = Pe^{-1/2}. \tag{3.26}$$

Rescaling of the z coordinate,

$$\mathfrak{z} = \frac{z}{2\cos\phi}, \tag{3.27}$$

leads to a diffusion equation of the form

$$\frac{\partial^2 P_2^{BL}}{\partial \zeta^2} - \frac{\partial P_2^{BL}}{\partial \mathfrak{z}} = 0. \tag{3.28}$$

The 'initial condition' $P_2^{BL}(\zeta, \mathfrak{z} = 0)$ for $\zeta > 0$ $(s > 2)$ is provided by the solution obtained in the previous section for $\tau \longrightarrow \infty$ (3.23) and for $\zeta < 0$ $(s < 2)$ the probability density function P_2^{BL} vanishes due to the absorbing boundary condition at the sphere. In the latter case the curvature of the boundary should, in principle, be taken into account; however, it influences the boundary condition only at higher orders, thus at leading order $P_2^{BL}(\zeta < 0, \mathfrak{z} = 0) = 0$. To obtain the 'initial condition' $P_2^{BL}(\zeta, \mathfrak{z} = 0)$ for $\zeta > 0$ explicitly first we need the explicit form of (3.23) in the suitable contracted boundary layer variables, i.e. $\zeta_c = (s-2)Pe^{2/3}$ and $\mathfrak{z}_c = zPe^{1/3}/2\cos\phi$. The relations between the variables (κ, τ) and $(\zeta_c, \mathfrak{z}_c)$ are

$$\kappa = \left(\zeta_c + \mathfrak{z}_c^2 \cos^2\phi\right)\cos^{2/3}\phi, \quad \tau = \mathfrak{z}_c \cos^{4/3}\phi, \tag{3.29a,b}$$

hence (3.23) can be transformed into

$$\frac{1}{2}\mathrm{erfc}\left(\frac{\tau^2 - \kappa}{\sqrt{4\tau}}\right) = \frac{1}{2}\mathrm{erfc}\left(-\frac{\zeta_c}{\sqrt{4\mathfrak{z}_c}}\right). \tag{3.30}$$

Now, returning to the original variables $(\xi, \mathfrak{z})$ we obtain

$$\frac{1}{2}\mathrm{erfc}\left(-\frac{\zeta_c}{\sqrt{4\mathfrak{z}_c}}\right) = \frac{1}{2}\mathrm{erfc}\left(-\frac{\zeta}{\sqrt{4\mathfrak{z}}}\right) \xrightarrow{\mathfrak{z}\to 0} 1. \tag{3.31}$$

Thus, the leading-order boundary condition at $\mathfrak{z} = 0$ takes the form

$$P_2^{BL}(\zeta, \mathfrak{z} = 0) = \begin{cases} 1 & \text{for } \zeta > 0, \\ 0 & \text{for } \zeta < 0. \end{cases} \tag{3.32}$$

The diffusion equation (3.28) can be solved by the use of the Green's formula

$$P_2^{BL}(\zeta, \mathfrak{z}) = \frac{1}{\sqrt{4\pi\mathfrak{z}}}\int_{-\infty}^{\infty} P_2^{BL}\left(\zeta', \mathfrak{z} = 0\right)\exp\left[-\frac{(\zeta-\zeta')^2}{4\mathfrak{z}}\right]\mathrm{d}\zeta' = \frac{1}{2}\mathrm{erfc}\left[-\frac{\zeta}{\sqrt{4\mathfrak{z}}}\right]. \tag{3.33}$$

Of course, the solution satisfies the boundary conditions, i.e. it tends to unity as $\zeta \longrightarrow \infty$ and to zero as $\zeta \longrightarrow -\infty$. By comparison of the solution (3.33) and the asymptotic form in (3.30) the matching with the layer at $\theta = \pi/2$ is correct.

3.1.4. *The lower boundary layer past the sphere*

To resolve the boundary layer that forms past the sphere in the vicinity of $x = 0$ and for $z < 0$ exists below the YZ plane whereas for $z > 0$ above it (cf. figure 1*a*), we return to the dimensional equation (2.3) with $\partial P_2^{BL}/\partial t = 0$, $\boldsymbol{V}(\boldsymbol{r}) = \boldsymbol{v}(\boldsymbol{r})$, $\boldsymbol{D}(\boldsymbol{r}) = D_0\boldsymbol{1}$ and use the standard variable transformation in the boundary layer theory introduced by von Mises (1927) and used, e.g., in Batchelor (1979),

$$\psi = \tfrac{1}{2}\dot{\gamma}x_*^2, \tag{3.34}$$

where ψ is the stream function of the shearing flow $\boldsymbol{v}(\boldsymbol{r})$ (cf. (2.4)) and the starred Cartesian coordinates are dimensional. We also introduce a new variable in place of z_*,

$$\lambda = \sqrt{2}D_0\dot{\gamma}^{1/2}\left(z_* \pm \sqrt{4 - y_*^2}\right), \tag{3.35}$$

where the $+$ sign corresponds to the layer that forms for $z < 0$ and the $-$ sign to the layer that forms for $z > 0$. The standard boundary layer theory allows one to arrive at a conclusion that the only two important terms in (3.1) which determine the structure of this boundary layer are the advective term $x\partial_z P_2^{BL}$ and the second x-derivative (and the boundary layer thickness is $\delta \sim Pe^{-1/3}$). Therefore, in the new variables (ψ, λ) the boundary layer equation for the pair probability density function takes the form

$$\frac{\partial P_2^{BL}}{\partial \lambda} = \frac{\partial}{\partial \psi}\left(\psi^{1/2}\frac{\partial P_2^{BL}}{\partial \psi}\right), \tag{3.36}$$

and the natural boundary conditions are such that

$$P_2^{BL}(\psi = 0) = 1, \quad P_2^{BL}(\psi \longrightarrow \infty) = 0 \quad \text{and} \quad P_2^{BL}(\lambda = 0) = 0; \tag{3.37a–c}$$

therefore, they do not involve any dimensional constants. Hence, the solution must be a function solely of the dimensionless variable

$$\Xi = \frac{\psi^{1/2}}{\lambda^{1/3}}, \tag{3.38}$$

with the use of which (3.36) reduces to

$$\frac{\mathrm{d}^2 P_2^{BL}}{\mathrm{d}\Xi^2} + \frac{4}{3}\Xi^2 \frac{\mathrm{d}P_2^{BL}}{\mathrm{d}\Xi} = 0. \tag{3.39}$$

The solution has the form

$$P_2^{BL} = 1 - \frac{1}{K}\int_0^{\Xi} \exp\left(-\frac{4}{9}\Xi'^3\right)\mathrm{d}\Xi', \tag{3.40}$$

where $\Xi = 2^{-2/3}Pe^{1/3}x/(z \pm \sqrt{4-y^2})^{1/3}$ and $\int_0^{\Xi} \exp(-\frac{4}{9}\Xi'^3)\mathrm{d}\Xi'$ is one of the incomplete gamma functions; thus,

$$K = \int_0^{\infty} \exp\left(-\frac{4}{9}\Xi'^3\right)\mathrm{d}\Xi' \approx 1.170. \tag{3.41}$$

The solution (3.40) satisfies the boundary conditions (3.37) and, moreover, it has the property

$$P_2^{BL}\,(z \longrightarrow -\infty) = 1 \quad \text{for } x < 0, \tag{3.42a}$$

$$P_2^{BL}\,(z \longrightarrow \infty) = 1 \quad \text{for } x > 0. \tag{3.42b}$$

For the sake of completeness of the presented analysis we will now resolve the two remaining boundary layers numerically. First, we consider the boundary layer that forms on the half-circumference of the central sphere above the YZ plane for $z<0$ and below it for $z>0$ and matches the $\delta \sim Pe^{-1}$ boundary layer with the lower boundary layer past the sphere of thickness $\delta \sim Pe^{-1/3}$, which it penetrates to the depth $Pe^{-1/2}$ (cf. figure 1*a*). The last remaining boundary layers are the ones at both sides (in the y direction) of the lower boundary layer past the sphere of thickness $\delta \sim Pe^{-1/3}$, which match this layer to the mainstream value $P_2^M = 1$ (cf. figure 1*b*).

3.1.5. *The half-circumference boundary layer at the YZ plane*

For this layer we have

$$\delta = Pe^{-1/2}, \quad \delta_\phi = Pe^{-1/2}, \tag{3.43a,b}$$

and thus the boundary layer equation takes the form

$$\phi \sin 2\theta\, \partial_\xi P_2^{BL} - \partial_\xi^2 P_2^{BL} - \frac{1}{4\sin^2\theta}\partial_\phi^2 P_2^{BL} = 0, \tag{3.44}$$

with boundary conditions resulting from the absorbing condition at the central sphere ($\xi = 0$), matching with the mainstream solution ($\xi \to \infty$, $\phi > 0$ for $z<0$ and $\phi < 0$ for $z>0$), matching with the lower boundary layer past the sphere of thickness $\delta \sim Pe^{-1/3}$ ($\phi \to -\infty$ at constant ξ and $\xi \to \infty$ at constant ϕ for $z<0$, and $\phi \to \infty$ at constant ξ and $\xi \to \infty$ at constant ϕ for $z>0$) and matching with the $\delta \sim Pe^{-1}$ boundary layer ($\phi \to \infty$ for $z<0$ and $\phi \to -\infty$ for $z>0$),

$$P_2^{BL}(\xi = 0, \phi) = 0, \quad P_2^{BL}\,(\xi \to \infty, \phi) = 1, \tag{3.45a}$$

$$P_2^{BL}(\xi, \phi \to -\infty) = 0, \quad P_2^{BL}\,(\xi, \phi \to \infty) = 1. \tag{3.45b}$$

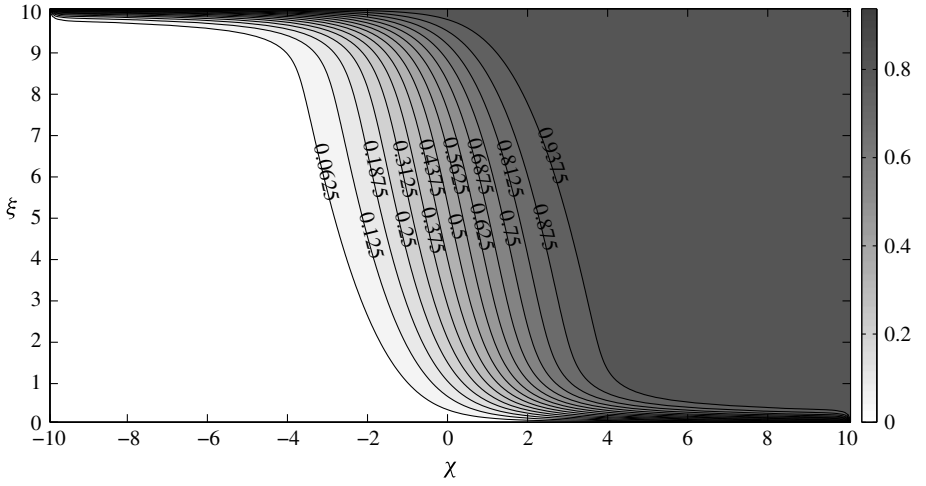

FIGURE 2. The grey-scale map and contour lines of the probability density function in the half-circumference boundary layer at the YZ plane; the numerical solution of (3.47) with the boundary conditions (3.48).

A change of variables

$$\varsigma = \sqrt{\mp\cos\theta}\,\xi, \quad \chi = \pm 2\sin\theta\sqrt{\mp\cos\theta}\,\phi, \tag{3.46a,b}$$

where the plus sign under the square root corresponds to the layer that forms for $z>0$ and the minus sign under the square root to the layer that forms for $z<0$, allows one to transform (3.44) into

$$\chi\,\partial_\varsigma P_2^{BL} + \partial_\varsigma^2 P_2^{BL} + \partial_\chi^2 P_2^{BL} = 0. \tag{3.47}$$

To fix ideas let us consider the region $z<0$, $y<0$ (or, equivalently, $z>0$, $y<0$), where the boundary conditions take the form

$$P_2^{BL}(\varsigma=0,\,\chi)=0, \quad P_2^{BL}(\varsigma\to\infty,\,\chi)=1, \tag{3.48a}$$
$$P_2^{BL}(\varsigma,\,\chi\to-\infty)=0, \quad P_2^{BL}(\varsigma,\,\chi\to\infty)=1. \tag{3.48b}$$

The numerical solution of (3.47) with the boundary conditions (3.48) is presented in figure 2.

3.1.6. *The side boundary layers at* $y=\pm 2$

In this case we have

$$\delta_x = \delta_y = Pe^{-1/3} \tag{3.49}$$

and the boundary layer equation is

$$\xi_x\partial_z P_2^{BL} - \partial_{\xi_x}^2 P_2^{BL} - \partial_{\xi_y}^2 P_2^{BL} = 0, \tag{3.50}$$

where

$$\xi_x = \frac{x}{\delta_x}, \quad \xi_y = \frac{y}{\delta_y}. \tag{3.51a,b}$$

For definiteness let us consider now the side boundary layer in the region $x>0$, $y>0$ and $z>0$. The boundary conditions result from matching with the mainstream solution at $\xi_x=0$ (ξ_y, z fixed), $\xi_y\to\infty$ (ξ_x, z fixed) and $z\to\infty$ (ξ_x, ξ_y fixed), matching with the upper boundary layer past the sphere of thickness $\delta\sim Pe^{-1/2}$ at $\xi_x\to\infty$ and with the lower boundary layer past the sphere of thickness $\delta\sim Pe^{-1/3}$ at $\xi_y\to-\infty$,

$$P_2^{BL}(\xi_x=0,\,\xi_y,\,z)=1, \tag{3.52a}$$

$$P_2^{BL}(\xi_x\longrightarrow\infty,\,\xi_y<0,\,z)=0, \tag{3.52b}$$

$$P_2^{BL}(\xi_x\longrightarrow\infty,\,\xi_y>0,\,z)=1, \tag{3.52c}$$

$$P_2^{BL}\left(\xi_x,\,\xi_y\to\infty,\,z\right)=1, \tag{3.52d}$$

$$P_2^{BL}(\xi_x,\,\xi_y\to-\infty,\,z)=1-\frac{1}{K}\int_0^{\xi_x/(4z)^{1/3}}\exp\left(-\frac{4}{9}\Xi'^3\right)\mathrm{d}\Xi', \tag{3.52e}$$

$$P_2^{BL}\left(\xi_x,\,\xi_y,\,z\to\infty\right)=1. \tag{3.52f}$$

Based on the dimensional analysis presented in 3.1.4, we propose to reduce the number of independent variables by the following change of variables:

$$\mu=\frac{x}{(4z)^{1/3}},\qquad \nu=\frac{y}{(4z)^{1/3}}. \tag{3.53a,b}$$

Equation (3.50) now takes the form

$$\tfrac{4}{3}\mu^2\partial_\mu P_2^{BL}+\tfrac{4}{3}\mu\nu\partial_\nu P_2^{BL}+\partial_\mu^2 P_2^{BL}+\partial_\nu^2 P_2^{BL}=0 \tag{3.54}$$

and the boundary conditions (3.52) transform into

$$P_2^{BL}\,(\mu=0,\,\nu)=1,\quad P_2^{BL}\,(\mu\to\infty,\,\nu<0)=0,\quad P_2^{BL}\,(\mu\to\infty,\,\nu>0)=1, \tag{3.55a}$$

$$P_2^{BL}\,(\mu,\,\nu\to\infty)=1,\quad P_2^{BL}(\mu,\,\nu\to-\infty)=1-\frac{1}{K}\int_0^{\mu}\exp\left(-\frac{4}{9}\mu'^3\right)\mathrm{d}\mu'. \tag{3.55b}$$

The numerical solution of the boundary layer equation (3.54) with the boundary conditions (3.55) is presented in figure 3. It can be seen that on the external side $y>2$ the layer is, in fact, very weak. In the vicinity of $z=0$ this layer extends to $-z\sim Pe^{-1/5}$, where the other length scales change to $\delta_x=\delta_y=Pe^{-2/5}$ and where it matches with the half-circumference boundary layer at the YZ plane from the previous section.

3.2. *Flocculation with hydrodynamic interactions*

The hydrodynamic interactions between the spheres are included through the non-trivial tensor functions $\boldsymbol{\mathcal{D}}(\boldsymbol{r})$ and $\boldsymbol{C}(\boldsymbol{r})$, which can be found, e.g., in Russel *et al.* (1989). The common level of approximation for the hydrodynamic interactions corresponds to the so-called Rotne–Prager–Yamakawa approximation (cf. Rotne & Prager 1969 and Yamakawa 1970), within which the flow obtained by introducing a sphere into the shear flow $\boldsymbol{v}(\boldsymbol{r})$ (cf. (2.4)), say $\boldsymbol{v}_1(\boldsymbol{r})$, is used to calculate the velocity $\boldsymbol{V}(\boldsymbol{r})$ of another sphere, introduced into the new flow $\boldsymbol{v}_1(\boldsymbol{r})$. We start at this level and then generalize in § 3.2.1. For the Rotne–Prager–Yamakawa case we have

$$\boldsymbol{C}(\boldsymbol{r})=\left[5\left(\frac{a}{r}\right)^3-8\left(\frac{a}{r}\right)^5\right]\hat{\boldsymbol{r}}\hat{\boldsymbol{r}}+\frac{16}{3}\left(\frac{a}{r}\right)^5(\boldsymbol{1}-\hat{\boldsymbol{r}}\hat{\boldsymbol{r}}), \tag{3.56}$$

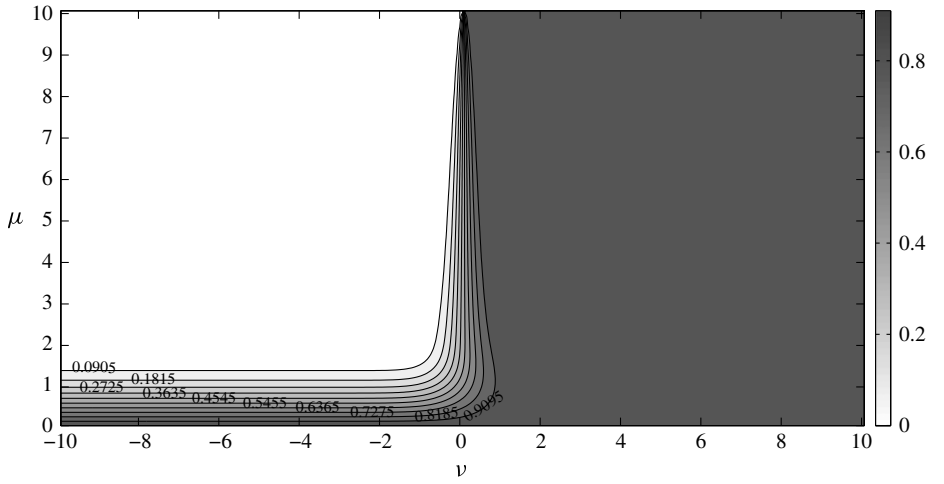

FIGURE 3. The grey-scale map and contour lines of the probability density function in the side boundary layer at $y=2$, $z>0$; the numerical solution of (3.54) with the boundary conditions (3.55).

so that

$$U_r = \left(r - \frac{5}{r^2} + \frac{8}{r^4}\right) \sin\theta \cos\theta \cos\phi, \tag{3.57a}$$

$$U_\theta = \left(-r + \frac{16}{3r^4}\right) \sin^2\theta \cos\phi - \frac{8}{3r^4} \cos\phi, \tag{3.57b}$$

$$U_\phi = \frac{8}{3r^4} \cos\theta \sin\phi \tag{3.57c}$$

and

$$\boldsymbol{\mathcal{D}}(\boldsymbol{r}) = D^{\parallel}(r)\hat{\boldsymbol{r}}\hat{\boldsymbol{r}} + D^{\cdot}(r)\left(\mathbf{1} - \hat{\boldsymbol{r}}\hat{\boldsymbol{r}}\right), \tag{3.58}$$

$$D^{\parallel}(r) = 1 - \frac{3}{2r} + \frac{1}{r^3}, \quad D^{\perp}(r) = 1 - \frac{3}{4r} - \frac{1}{2r^3}, \tag{3.59}$$

where (r, θ, ϕ) are the usual spherical coordinates. Hence,

$$\boldsymbol{\nabla} \cdot [\boldsymbol{\mathcal{D}} \cdot \boldsymbol{\nabla} P_2] = \frac{1}{r^2}\frac{\partial}{\partial r}\left(r^2 D^{\parallel}(r)\frac{\partial P_2}{\partial r}\right) + \frac{D^{\perp}(r)}{r^2}\mathcal{L}^2_{\theta,\phi} P_2, \tag{3.60}$$

where

$$\mathcal{L}^2_{\theta,\phi} = \frac{1}{\sin\theta}\frac{\partial}{\partial\theta}\left(\sin\theta\frac{\partial}{\partial\theta}\right) + \frac{1}{\sin^2\theta}\frac{\partial^2}{\partial\phi^2}. \tag{3.61}$$

In the limit of large Péclet number, $Pe \gg 1$, the mainstream problem outside all the boundary layers is dominated by advection; thus, at leading order (cf. (2.7))

$$\boldsymbol{U} \cdot \boldsymbol{\nabla} P_2^M = 0, \tag{3.62}$$

so that the mainstream solution is constant on the streamlines of $\boldsymbol{U}(\boldsymbol{r})$. Since the far-field boundary condition is $P_{2,I}^{M}(r \longrightarrow \infty) = 1$ we obtain

$$P_{2,I}^{M} = 1 \tag{3.63}$$

in the mainstream region, where the streamlines span to infinity. To establish the region of validity of the above mainstream solution one must find the streamlines of the velocity field $\boldsymbol{U}(\boldsymbol{r})$ given in (3.57). These are found numerically and depicted in figure 4. Clearly, two types of significantly different regions can be identified, region II in the figure, where, at least in part of the region, the streamlines emerge from the sphere, reverse on the *YZ* plane and then come back to the sphere, and region I, where the streamlines span to infinity (some of them hitting the sphere). These two regions are separated by critical streamlines (surfaces) and boundary layers must necessarily form along them. Since the pair probability density function vanishes at the sphere, it must vanish in the entire region II and thus must be matched through a boundary layer along the critical streamlines to the mainstream solution (3.63). On one side the critical streamline is the one that is tangent to the sphere at $\theta = \pi/2$. (In fact, just as in the case without hydrodynamic interactions at $\theta = \pi/2$, the normal component of the velocity vanishes, implying singularity in the boundary layer. The boundary layer at ($r = 2$, $\theta = \pi/2$) of thickness $\delta = Pe^{-2/3}$ and meridional span $\delta_{\vartheta} = Pe^{-1/3}$ could, in fact, be solved by the introduction of new variables $\tau' = (25Pe\cos\phi/44)^{1/3}\,(\pi/2 - \theta)$ and $\kappa' = (55/54)^{1/3}(Pe\cos\phi)^{2/3}\,(r-2)$ in place of τ and κ and then by proceeding exactly as in § 3.1.2.) On the other side the critical streamline starts at infinity and hits the sphere at some $|x_C| < 2a$ (point C in figure 4) and all other streamlines that are closer to the *YZ* plane reverse at that plane. The existence of such a streamline can be shown analytically in the asymptotic regime $|z| \gg 1$ and $|x| \ll 1/|z| \ll 1$, where the velocity field $\boldsymbol{U}$ can be approximated by $U_x \approx -8/3z^4$, $U_z \approx x$ (and $U_y \approx -15xy/3z^4$) and thus the asymptotic form of the streamlines on planes $y = \text{const.}$ is described by $x^2 = \text{Const}_y + 16/9|z|^3$. The critical streamline is that for $\text{Const}_y = 0$, since for any $\text{Const}_y < 0$ the streamline must reverse at $x = 0$, whereas for $\text{Const}_y > 0$ it spans to infinity. The surface bounding the region of closed streamlines was found by Batchelor & Green (1972) to be axisymmetric about the x axis.

The $\delta = Pe^{-1}$ boundary layer still forms at the sphere, but now only in the region I, since only in that region is the mainstream solution $P_{2,I}^{M} = 1$ and are strong gradients formed at the sphere to adjust the solution to the boundary condition. To resolve this boundary layer we introduce the boundary layer variable $\xi = (r-2)/\delta$, and as before, due to the symmetry of the problem, it is sufficient to concentrate on the upper half-sphere $-\pi/2 \leqslant \phi \leqslant \pi/2$ (and then the solution for the lower half-sphere can be easily reproduced). Outside the neighbourhood of ($r = 2$, $\theta = \pi/2$), ($r = 2$, $x = x_C$) and ($r = 2$, $\phi = \pm\pi/2$) the distinguished balance in the boundary layer includes the dominant advective term and the dominant diffusive term, and thus yields

$$\frac{10}{3}\sin\theta\cos\theta\cos\phi\frac{\partial P_2^{BL}}{\partial\xi} - \frac{\partial^2 P_2^{BL}}{\partial\xi^2} = 0. \tag{3.64}$$

The solution satisfying the absorbing boundary condition on the sphere, $P_2(r = 2) = P_2^{BL}(\xi = 0) = 0$, and matching with the mainstream solution as $\xi \longrightarrow +\infty$ is

$$P_2^{BL} = 1 - \mathrm{e}^{(U_{r0}/D_0^{\parallel})\xi} = 1 - \mathrm{e}^{5/3\sin 2\theta\cos\phi\xi}, \tag{3.65}$$

where $U_{r0}/D_0^{\parallel} = (10/3)\sin\theta\cos\theta\cos\phi$ is the ratio of the radial velocity component to the diffusion component $D^{\parallel}$ at the surface of the sphere. Precise calculation of

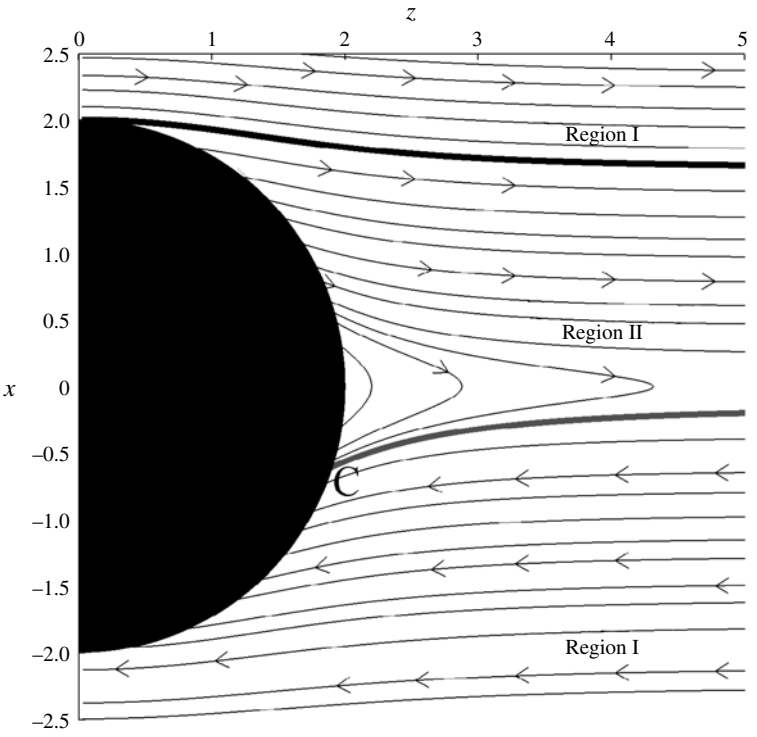

FIGURE 4. The numerically computed streamlines of the flow $\boldsymbol{U}(\boldsymbol{r})$ given in (3.57) in the XZ plane. The bold lines indicate the critical streamlines along which boundary layers form and which separate regions with different mainstream solutions. The black bold line for $x > 0$ is tangent to the sphere in the XY plane and for $z > 0$ indicates a boundary layer that forms past the sphere in the flow. The bold grey line for $x < 0$ indicates the numerically estimated position of a streamline below which the particles from infinity are hitting the central sphere and above which the concentration is zero (cf. figure 5 in Zinchenko & Davis (1995)); below its point of contact with the sphere, denoted by C, a boundary layer of thickness $\delta \sim Pe^{-1}$ forms at the sphere.

the leading-order average flux towards the central particle requires knowledge of the limits of integration at the surface of the sphere, i.e. the part of the sphere surface in contact with region I. However, for the present purposes it is sufficient to provide the following upper bound on the value of the coagulation rate (average flux), by performing the integration over the entire region $\pi/2 < \theta < \pi$, $-\pi/2 < \phi < \pi/2$ and $0 < \theta < \pi/2$, $\pi/2 < \phi < 3\pi/2$, as in the previous case without hydrodynamic interactions, which yields

$$\begin{aligned} J_{\text{with HI}} &< -8D_0c_0a\int_{-\pi/2}^{\pi/2}\mathrm{d}\phi\int_{\pi/2}^{\pi}\mathrm{d}\theta\,\sin\theta D^{\parallel}\left.\frac{\partial P_2}{\partial r}\right|_{r=2} \\ &= -3PeD_0c_0a\int_{-\pi/2}^{\pi/2}\mathrm{d}\phi\int_{\pi/2}^{\pi}\mathrm{d}\theta\,\sin\theta\left.\frac{\partial P_2^{BL}}{\partial \xi}\right|_{\xi=0} \\ &= 10PeD_0c_0a\int_{-\pi/2}^{\pi/2}\mathrm{d}\phi\int_{\pi/2}^{\pi}\mathrm{d}\theta\,\sin^2\theta\cos\theta\cos\phi = -\tfrac{20}{3}PeD_0c_0a, \end{aligned} \quad (3.66)$$

a value 0.625 times smaller than the result obtained in the absence of hydrodynamic interactions in (3.12). The actual rate of aggregation is even smaller, as indicated by the inequality in (3.66). It can be computed directly using, e.g., the approach of Batchelor & Green (1972) (cf. their (6.9) and (3.74) in this paper with $\epsilon = 0$), which allows one to estimate the value of the x coordinate of point C in figure 4, $x_C = 0.5757$. This, in turn, leads to

$$J_{\text{with HI}} = -\frac{20}{3}\left[1 - \left(\frac{x_C}{2}\right)^2\right]^{3/2} PeD_0c_0a \approx 5.86PeD_0c_0a, \tag{3.67}$$

which is approximately 55 % of the coagulation rate in the absence of hydrodynamic interactions.

3.2.1. *Generalization of the hydrodynamic interactions*

The results can be very easily generalized to any form of two-particle mobility functions. However, to include the near-field dynamics (i.e. the lubrication corrections) one needs to set the surface of pair formation, where the irreversible flocculation occurs, away from $r = 2$, since the relative particle mobility vanishes at $r = 2$ in such a case. This corresponds to the introduction of a simplest interaction potential, i.e. to the imposition of the following flocculation condition:

$$P_2(r = 2 + \epsilon) = 0, \tag{3.68}$$

where ϵ is a dimensionless parameter, denoting the ratio of the radial distance between the surface $r = 2$ and the surface of flocculation to the particle radius a, typically much smaller than unity. The general form of the shear disturbance tensor is (cf. e.g. Zinchenko & Davis 1995)

$$\boldsymbol{C}(\boldsymbol{r}) = A(r)\hat{\boldsymbol{r}}\hat{\boldsymbol{r}} + B(r)(\boldsymbol{1} - \hat{\boldsymbol{r}}\hat{\boldsymbol{r}}). \tag{3.69}$$

The degree of strength of the hydrodynamic interactions can now be easily tuned with the choice of functions $A(r)$, $B(r)$, $D^{\parallel}(r)$ and $D^{\perp}(r)$ (see (3.58)), which can be found in Russel *et al.* (1989) or Wang, Zinchenko & Davis (1994). This leads to

$$U_r = (1 - A)r\sin\theta\cos\theta\cos\phi, \tag{3.70a}$$

$$U_\theta = (-1 + B)\,r\sin^2\theta\cos\phi - \tfrac{1}{2}Br\cos\phi, \tag{3.70b}$$

$$U_\phi = \tfrac{1}{2}Br\cos\theta\sin\phi. \tag{3.70c}$$

To include the near-field dynamics ($1 - A \sim r - 2$; $D^{\parallel} \sim r - 2$) we assume at this point $\epsilon \gg Pe^{-1}$, so that the dominant $\delta = Pe^{-1}$ boundary layer balance between radial advection and radial diffusion holds. Introducing

$$\xi = [r - (2 + \epsilon)]Pe, \tag{3.71}$$

similarly to (3.65),we arrive at

$$P_2^{BL} = 1 - \mathrm{e}^{(U_{r0}/D_0^{\parallel})\xi} = 1 - \exp(((1 - A_0)/D_0^{\parallel})(2 + \epsilon)\sin\theta\cos\theta\cos\phi\xi), \tag{3.72}$$

where the subscript 0 denotes a value taken at $\xi = 0$, i.e. $r = 2 + \epsilon$. The flocculation rate can now be calculated in an analogous way to (3.67),

$$J_{\text{with HI}} = -\frac{4}{3}(2+\epsilon)^3 (1 - A_0) \left[1 - \left(\frac{x_C}{2}\right)^2\right]^{3/2} PeD_0 c_0 a, \tag{3.73}$$

and x_C is the x coordinate of the point of intersection between the critical streamline bounding the region of closed streamlines and the pair formation surface at $r = 2 + \epsilon$. We rewrite here the formula for x_C from Batchelor & Green (1972) for the convenience of the reader,

$$x_C^2 = \exp\left[2\int_{2+\epsilon}^{\infty} \frac{A(r) - B(r)}{1 - A(r)} \frac{\mathrm{d}r}{r}\right] \int_{2+\epsilon}^{\infty} \frac{rB(r)}{1 - A(r)} \exp\left[-2\int_{r}^{\infty} \frac{A(r') - B(r')}{1 - A(r')} \frac{\mathrm{d}r'}{r'}\right] \mathrm{d}r. \tag{3.74}$$

With the use of the above formulae (3.73) and (3.74) we can easily reproduce the results of the previous sections. By setting $A(r) = B(r) = \epsilon = 0$ we obtain the result for the case of no hydrodynamic interactions as in (3.12) and by setting the Rotne–Prager–Yamakawa mobility functions for $A(r)$ and $B(r)$ as in (3.56) and $\epsilon = 0$ we reproduce the result in (3.67). Finally, we compare the expression for the flux obtained in (3.73) with the flux in the case without hydrodynamic interactions but as in the current considerations with the flocculation surface set at a distance ϵ from the sphere $r = 2$,

$$\frac{J_{\text{with HI}}}{J_{\text{no HI}}} = (1 - A_0) \left[1 - \left(\frac{x_C}{2}\right)^2\right]^{3/2} < 1. \tag{3.75}$$

This clearly shows that the effect of hydrodynamic interactions on the movements of spherical particles in a shearing flow is detrimental to the rate of Brownian flocculation. However, it is not the only effect, which needs to be taken into account when the hydrodynamic interactions are considered. In the limit of large Pe analysed the diffusion has very little effect on the coagulation process, but hydrodynamic interactions influence the diffusion significantly. To determine the influence of the hydrodynamic interactions on the full coagulation process one must also see how the rate of coagulation is affected by non-trivial diffusion. In the next section we show that the other effect, i.e. the influence of non-trivial diffusion for hydrodynamically interacting particles, is also detrimental to the coagulation process.

4. Limit of small Péclet number, $Pe \ll 1$

We will briefly review the solution for the small Péclet number limit in the absence of hydrodynamic interactions, which is essentially the same as that of Frankel & Acrivos (1968) for $q(\boldsymbol{r}) = 1 - P_2(\boldsymbol{r})$. Since the diffusion significantly decreases with decreasing interparticle distances, it is naturally expected that the hydrodynamic interactions should weaken the flocculation process for $Pe \ll 1$. The perturbative problem for small Péclet number is singular since the term $Pex\partial_z P_2$ in (3.1) is negligible only for $r \ll Pe^{-1/2}$ and for $r \sim Pe^{-1/2}$ becomes comparable with the diffusion term. Therefore, following Frankel & Acrivos (1968) we use the method of matched asymptotic expansions and we divide the domain into two regions, the inner region, $2 < r \ll Pe^{-1/2}$, where diffusion dominates, and the outer region, $r \sim Pe^{-1/2}$, where the advection and diffusion are comparable, and expand in the

following perturbative series:

$$q(r,\theta,\phi) = q_0(r,\theta,\phi) + \sum_{n=1}^{\infty} f_n(Pe) q_n(r,\theta,\phi) \quad \text{in the inner region,} \tag{4.1a}$$

$$Q(R,\theta,\phi) = \sum_{n=0}^{\infty} F_n(Pe) Q_n(r,\theta,\phi) \quad \text{in the outer region,} \tag{4.1b}$$

where the outer variable $\boldsymbol{R} = Pe^{1/2}\boldsymbol{r}$ and the solutions from both regions must be matched for $1 \ll r \ll Pe^{-1/2}$. The problem in the outer region at leading order takes the form

$$X\partial_Z Q_0 - \nabla^2_{\boldsymbol{R}} Q_0 = 0. \tag{4.2}$$

The Green's function for this equation, thus the solution that vanishes at infinity (i.e. for $r \gg Pe^{-1/2}$) and behaves as $2/R + \text{Const.}$ for $R \ll 1$ (i.e. for $r \ll Pe^{-1/2}$), following Elrick (1962) and Frankel & Acrivos (1968) has the form

$$Q_0(\boldsymbol{R}) = \frac{1}{\sqrt{\pi}} \int_0^{\infty} \frac{\mathrm{d}s}{\left(1 + s^2/12\right)^{1/2} s^{3/2}} \exp\left\{ -\left[\frac{(X - sY/2)^2}{4s\left(1 + s^2/12\right)} + \frac{Y^2 + Z^2}{4s} \right] \right\}. \tag{4.3}$$

Indeed, for $R \ll 1$ we obtain

$$Q_0(R) \approx \frac{2}{R} + \frac{k}{\sqrt{\pi}}, \quad \text{with } k = \int_0^{\infty} \frac{\mathrm{d}s}{s^{3/2}} \left[\left(1 + s^2/12\right)^{-1/2} - 1 \right] \approx -0.9104. \tag{4.4}$$

(We divide the integral in (4.3) into two integrals $\int_0^{\varepsilon} + \int_{\varepsilon}^{\infty}$, where $\varepsilon \ll 1$ is an arbitrary constant. We can then expand the integrand under the first integral for small s and the second integral is convergent for $\boldsymbol{R} = 0$.) On the other hand, since the inner solution has to satisfy spherically symmetric boundary conditions it also has to be spherically symmetric at least up to the order defined by $f_1(Pe)$, hence

$$q(r) = \frac{2}{r} + f_1(Pe)\left(1 - \frac{2}{r}\right) + \cdots. \tag{4.5}$$

The two solutions can be matched in the region $1 \ll r \ll Pe^{-1/2}$ for

$$F_0(Pe) = Pe^{1/2} \quad \text{and} \quad f_1(Pe) = \frac{k}{\sqrt{\pi}} Pe^{1/2}. \tag{4.6a,b}$$

Therefore, the total dimensional flux takes the form (by integrating over the surface $r = 2$)

$$\begin{aligned} J_{\text{no HI, small } Pe} &= 4D_0 c_0 a \int_0^{2\pi} \mathrm{d}\phi \int_0^{\pi} \mathrm{d}\theta \sin\theta \left.\frac{\partial q}{\partial r}\right|_{r=2} \\ &= -8\pi D_0 c_0 a \left(1 - \frac{k}{\sqrt{\pi}} Pe^{1/2}\right) + \mathrm{O}(Pe), \end{aligned} \tag{4.7}$$

where $k \approx -0.9104$, so that the correction resulting from the presence of the shear flow increases the flux towards the central particle.

Next, if we switch on the hydrodynamic interactions according to (3.56)–(3.59), the outer problem for $Q_{HI\,0}(R)$ remains unchanged and the only thing that changes is the inner solution for $q_{HI}(r)$, which is now

$$q_{HI}(r) = 1 - \frac{\displaystyle\int_2^r \frac{\mathrm{d}r'}{r'^2 D^{\parallel}(r')}}{\displaystyle\int_2^\infty \frac{\mathrm{d}r}{r^2 D^{\parallel}(r)}}. \tag{4.8}$$

Since $D^{\parallel}(r)$ satisfies $0 < D^{\parallel}(r) < 1$ for all $r > 2$, we obtain

$$\int_2^\infty \frac{\mathrm{d}r}{r^2 D^{\parallel}(r)} > \int_2^\infty \frac{\mathrm{d}r}{r^2} = \frac{1}{2}, \tag{4.9}$$

which means that the aggregation rate satisfies

$$\begin{aligned} J_{\text{with HI, small } Pe} &= 4D_0 c_0 a \int_0^{2\pi} \mathrm{d}\phi \int_0^{\pi} \mathrm{d}\theta \sin\theta \; D^{\parallel} \frac{\partial q_{HI}}{\partial r}\bigg|_{r=2} \\ &= \frac{1}{2\displaystyle\int_2^\infty \frac{\mathrm{d}r}{r^2 D^{\parallel}(r)}} J_{\text{no HI, small } Pe} < J_{\text{no HI, small } Pe} \end{aligned} \tag{4.10}$$

(direct numerical computation of the integral in the second line of (4.10) leads to a more exact relation $J_{\text{with HI, small } Pe} \approx 0.6 J_{\text{no HI, small } Pe}$). Therefore, as expected, in the limit of small Pe the hydrodynamic interactions slow down the flocculation process, similarly to what was reported for $Pe \gg 1$.

A generalization analogous to the large Pe number limit is easily made here by changing the lower limits of the integrals in (4.8) from 2 to $2+\epsilon$.

5. Concluding remarks

The problem of the influence of hydrodynamic interactions on the process of Brownian flocculation in external shear flow has been investigated in detail.

First, the problem without hydrodynamic interactions, as defined by (3.1) and (2.9), has been solved in the limit of large Pe number. A complete solution for the spatial distribution of the pair probability density function $P_2(\boldsymbol{r})$ has been provided by use of boundary layer theory and the regularizing effect of the potentials of interaction between particles, such as van der Waals or Lennard-Jones potentials, has been ignored. The limit of vanishing hydrodynamic interactions turned out to be very singular; the structure of the solution exhibits a number of different length scales, as depicted in figure 1. The thinnest boundary layer, of thickness $\delta \sim Pe^{-1}$, allows one to calculate the flocculation rate at leading order, which agrees with the known ballistic result of Levich (1962). Other length scales present in the system are $Pe^{-1/3}$, $Pe^{-1/2}$ and $Pe^{-2/3}$ and there are six different boundary layer types in the distribution of $P_2(\boldsymbol{r})$, which are all resolved here.

Next, the hydrodynamic interactions were included in the problem. First, the well-known Rotne–Prager–Yamakawa approximation (cf. Rotne & Prager 1969; Yamakawa 1970 and Russel *et al.* 1989) was exploited. In the limit of large Pe number the analysis of the thinnest, $\delta \sim Pe^{-1}$, boundary layer allowed us to find the flocculation rate and prove that, since the hydrodynamic interactions diverge the

streamlines hitting the central sphere, they weaken the Brownian flocculation process, and thus the rate of flocculation is decreased by approximately 55 %. The structure of the $P_2(\boldsymbol{r})$ distribution is still quite singular in this case (see figure 4 and comments below), and there are still boundary layers that span from the sphere surface to infinity. The hydrodynamic interactions were then generalized to an arbitrary form of the two-particle mobility functions, with the flocculation surface shifted by an arbitrary distance ϵ from the central sphere, i.e. $P_2(r = 2 + \epsilon) = 0$, to take into account the near-field dynamics (lubrication). A simple explicit final expression for the flocculation rate was obtained, and the detrimental effect of hydrodynamic interactions was confirmed. Finally, the limit of small *Pe* number was also considered and it was demonstrated, perhaps not surprisingly in this case, that the inclusion of hydrodynamic interactions slows down the flocculation process.

To conclude, it was shown here that both effects, the divergence of streamlines hitting the central sphere and the decrease of diffusion with decrease of the interparticle distances, which result from hydrodynamic interactions between particles, are detrimental to the process of Brownian flocculation. (In other words, both components of the mobility matrix, typically denoted as $\boldsymbol{\mu}^{td}$ (translational–dipolar) and $\boldsymbol{\mu}^{tt}$ (translational–translational), slow down the flocculation process.)

Acknowledgements

I would like to thank Professor Eligiusz Wajnryb, Dr Piotr Szymczak and Pawel Zuk for fruitful discussions. I am also very grateful to the anonymous referee for fruitful comments, which helped to improve the final version of the manuscript. The financial support of the Polish National Science Centre (grant no. 2012/05/B/ST8/03010) is gratefully acknowledged.

Appendix A

Following Dormy *et al.* (2002), (3.19) determining the structure of the boundary layer at $r = 2$, $\theta = \pi/2$ has solutions in the form

$$\mathrm{e}^{\tau\lambda_1\sigma}\mathrm{Ai}(\lambda_1\sigma + \kappa), \quad \mathrm{e}^{\tau\lambda_2\sigma}\mathrm{Ai}(\lambda_2\sigma + \kappa), \quad \mathrm{e}^{\tau\lambda_3\sigma}\mathrm{Ai}(\lambda_3\sigma + \kappa), \tag{A 1}$$

where λ_j $(j = 1, 2, 3)$ and σ are the solution parameters, and Ai $(\cdot)$ is the Airy function. The identity

$$3\int_0^\infty \sigma^{3m}\mathrm{Ai}\,(\sigma)\,\mathrm{d}\sigma = \frac{(3m)!}{3^m m!} \quad \text{for } m = 0, 1, 2, 3, \ldots \tag{A 2}$$

can be used to derive the following relation:

$$\int_0^\infty \mathrm{Ai}(\sigma)[\exp(\omega^{-1}\tau\sigma) + \exp(\tau\sigma) + \exp(\omega\tau\sigma)]\mathrm{d}\sigma = \exp\left(\frac{1}{3}\tau^3\right), \tag{A 3}$$

where $\omega = \mathrm{e}^{2/3\pi\mathrm{i}}$ (1, ω and ω^{-1} are the cubic roots of unity).

The condition (3.20*b*) suggests $\lambda_1 = 1$, $\lambda_2 = \omega$ and $\lambda_3 = \omega^{-1}$; hence, the solution takes the form of the following linear combination of the terms given in (A 1):

$$\Psi = \Psi_{-1} + \Psi_0 + \Psi_1, \tag{A 4}$$

where

$$\Psi_n = \int_0^\infty \frac{\mathrm{Ai}(\sigma)\mathrm{Ai}(\kappa+\omega^n\sigma)}{\mathrm{Ai}(\omega^n\sigma)}\exp(\omega^n\tau\sigma)\mathrm{d}\sigma. \tag{A 5}$$

By the use of (A 3) this solution easily satisfies the boundary condition (3.20*b*). On the other hand, the asymptotic form of the Airy function for large arguments (cf. Abramowitz & Stegun 1972),

$$\mathrm{Ai}(z) \sim \frac{1}{2\pi^{1/2}z^{1/4}}\mathrm{e}^{-2z^{3/2}/3}\left[1-\frac{5}{48z^{3/2}}+\mathrm{O}\left(z^{-3}\right)\right], \quad \text{for } |z|\to\infty,\ |\arg z|<\pi, \tag{A 6}$$

demonstrates that the Airy functions decay exponentially for large and positive σ; thus, it is evident that the condition (3.20*a*) is also satisfied.

The asymptotic behaviour of the solution as $\tau\to-\infty$, although evident from (3.15) and (3.17), can also be found via the saddle point method. We direct the interested reader to Roberts (1967) and Dormy *et al.* (2002).

As a final step we find the asymptotic behaviour of the solution (A 4) and (A 5) for large and positive τ (which proves useful for matching with the upper boundary layer past the sphere of thickness $\delta\sim Pe^{-1/2}$). In this case the dominant contribution comes from Ψ_0, since $\mathrm{Re}(\omega^{-1})<0$ and $\mathrm{Re}(\omega)<0$. We will find its asymptotic form by use of the saddle point method.

By expanding the Airy functions in (A 5) up to the first order as in (A 6) for large σ one obtains

$$\Psi_0 \sim \int_0^\infty \frac{\exp\left[\gamma(\sigma)\right]}{\sqrt{4\pi}(\kappa+\sigma)^{1/4}}\mathrm{d}\sigma, \quad \text{for } \tau\gg 1, \tag{A 7}$$

where $\gamma(\sigma)=-2(\kappa+\sigma)^{3/2}/3+\sigma\tau$. The saddle point coordinate σ_s must satisfy

$$\gamma'(\sigma_s)=-(\kappa+\sigma_s)^{1/2}+\tau=0, \quad \Longrightarrow \quad \sigma_s=\tau^2-\kappa. \tag{A 8}$$

By substituting into $\gamma(\sigma_s)$ we obtain

$$\gamma(\sigma_s)\sim \tfrac{1}{3}\tau^3-\tau\kappa, \tag{A 9}$$

and since $\gamma''(\sigma_s)=-1/2\tau$, the asymptotic evaluation in the neighbourhood of the saddle leads to

$$\Psi_0 \sim \frac{1}{2}\exp\left(\frac{1}{3}\tau^3-\tau\kappa\right)\mathrm{erfc}\left(-\frac{\tau^2-\kappa}{\sqrt{4\tau}}\right). \tag{A 10}$$

Hence, the asymptotic (κ,τ)-dependence of the pair probability density function (3.18) as $\tau\to\infty$ is

$$P_2^{BL}(\kappa,\tau\gg 1)\sim 1-\frac{1}{2}\mathrm{erfc}\left(-\frac{\tau^2-\kappa}{\sqrt{4\tau}}\right)=\frac{1}{2}\mathrm{erfc}\left(\frac{\tau^2-\kappa}{\sqrt{4\tau}}\right). \tag{A 11}$$

REFERENCES

ABRAMOWITZ, M. & STEGUN, I. A. 1972 *Handbook of Mathematical Functions with Formulas, Graphs, and Mathematical Tables*. Dover Publications.

ACRIVOS, A. & TAYLOR, T. D. 1962 Heat and mass transfer from single spheres in Stokes flow. *Phys. Fluids* **5**, 387–394.

BATCHELOR, G. K. 1979 Mass transfer from a particle suspended in fluid with a steady linear ambient velocity distribution. *J. Fluid Mech.* **95**, 369–400.

BATCHELOR, G. K. & GREEN, J. T. 1972 The hydrodynamic interaction of two small freely-moving spheres in a linear flow field. *J. Fluid Mech.* **56**, 375–400.

DORMY, E., JAULT, E. & SOWARD, A. M. 2002 A super-rotating shear layer in magnetohydrodynamic spherical Couette flow. *J. Fluid Mech.* **452**, 263–291.

ELRICK, D. E. 1962 Source functions for diffusion in uniform shear flow. *Austral. J. Phys.* **15**, 283–288.

FRANKEL, N. A. & ACRIVOS, A. 1968 Heat and mass transfer from small spheres and cylinders freely suspended in shear flow. *Phys. Fluids* **11**, 1913–1918.

KIM, S. & KARRILA, S. J. 2005 *Microhydrodynamics. Principles and Selected Applications*. Dover Publications.

LEVICH, V. G. 1962 *Physiochemical Hydrodynamics*. Prentice-Hall.

VON MISES, R. 1927 Bemerkungen zur Hydrodynamik. *Z. Angew. Math. Mech.* **7**, 425–431.

NOH, D. S., KOH, Y. & KANG, I. S. 1998 Numerical solutions for shape evolution of a particle growing in axisymmetric flows of supersaturated solution. *J. Cryst. Growth* **183**, 427–440.

ROBERTS, P. H. 1967 Singularities of Hartmann layers. *Proc. R. Soc. Lond.* A **300**, 94–107.

ROTNE, J. & PRAGER, S. 1969 Variational treatment of hydrodynamic interaction in polymers. *J. Chem. Phys.* **50**, 4831–4837.

RUSSEL, W. B., SAVILLE, D. A. & SHOWALTER, W. A. 1989 *Colloidal Dispersions*. Cambridge University Press.

SMOLUCHOWSKI, M. 1917 Versuch einer mathematischen Theorie der Koagulationkinetik kolloider lösungen. *Z. Phys. Chem.* **92**, 129–168.

WANG, H., ZINCHENKO, A. Z. & DAVIS, R. H. 1994 The collision rate of small drops in linear flow fields. *J. Fluid Mech.* **265**, 161–188.

YAMAKAWA, H. 1970 Transport properties of polymer chains in dilute solution: hydrodynamic interaction. *J. Chem. Phys.* **53**, 436–443.

ZINCHENKO, A. Z. & DAVIS, R. H. 1995 Collision rates of spherical drops or particles in a shear flow at arbitrary Péclet numbers. *Phys. Fluids* **7**, 2310–2327.